Feedback impedance control for sound absorption with corona discharge actuator

Stanislav Sergeev[1], Hervé Lissek[1]

[1]Signal Processing Laboratory LTS2, EPFL, CH-1015 Lausanne, Switzerland
stanislav.sergeev@epfl.ch, herve.lissek@epfl.ch

Abstract

This paper introduces an application of a plasma-based actuator for active noise reduction problems. The actuator is based on an atmospheric corona discharge in a wire-to-mesh geometry. Its satisfactory electroacoustic characteristics and the absence of moving parts make the corona discharge actuator a serious alternative to conventional electrodynamic loudspeakers for active impedance control techniques. In this work, a pressure-velocity feedback impedance control strategy for active sound absorption adapted to corona discharge actuators is presented. Two approaches of particle velocity estimation with two microphones are considered. The first is based on the linear approximation of pressure gradient, the second measures flow velocity through an additional resistive layer in front of the actuator. The experimental validation is performed in an impedance tube under the normal sound incidence. According to the results, such a system with a corona discharge actuator as a controlled transducer can provide high sound absorption over a wide frequency range using any of the methods of velocity estimation.

Keywords: active noise control, sound absorption, corona discharge, plasma actuator.

1   Introduction

With recent advances in real-time digital controllers active sound control becomes a common solution for noise reduction problems in low and middle audio frequency ranges. Various techniques such as noise cancellation and impedance control find their applications in different areas [1]-[5]. The electrodynamic loudspeakers are commonly used as controlled sources to manipulate the sound field. Low cost, ease of implementation, frequency response and low distortion qualify these transducers as an optimal choice for many cases. However, in certain situations an alternative transducer may be preferred. For instance, implementation of active noise control systems in window panels requires transparency of the transducer. Although piezoelectric films are proposed [6], the polymer-based membrane can be fragile to a mechanical impact. Also, in the many cases where weight and available space are the main factors, such as acoustic liners [7][8], light, compact but still resistant to harsh environment solutions would be beneficial. Moreover, conventional loudspeakers have typically circular or elliptical membrane shape, whereas more flexibility in design might be needed in order to optimally cover a treated area in complex installations. Finally, electrodynamic loudspeaker presents a mechanical resonator which limits the absorption bandwidth in impedance control methods [9]. Thus, there is a great potential for active control methods to benefit from the alternative electroacoustic transducers that do not exhibit the abovementioned shortcomings.

Plasma-based transducers are considered as a possible candidate for active noise control applications. Extensively studied in the field of flow control [10], these actuators can also produce sound [11]. Sound generation results from direct transfer of mechanical momentum from ionized particles to the surrounding medium and a heat release from a discharge zone. Thus, without any moving parts, the plasma-based actuators

are simple in design and lightweight, have short response time to the input signal. In the previous work [12], the authors studied the transducer operating on the principle of the atmospheric corona discharge (CD). The analysis of basic acoustic characteristics such as frequency response, directivity, and harmonic distortion brought to the conclusion that the CD actuator is potentially suitable for active noise control. The follow-up work presented the implementation of the so-called "hybrid absorption method" with the use of CD actuators [13]. Although high and broadband absorption was achieved under normal incidence, the FxLMS based methods need the measurement of reference noise, which is not always available. Moreover, in this control strategy, the fixed resistance of a passive porous layer determines the target acoustic impedance. Thus, any change in impedance for optimal absorption, e.g. grazing sound incidence, requires a change of material, which is impractical. In this study, we design a feedback impedance control method, which relies on direct measurements of acoustic pressure and velocity. The target impedance for optimal absorption can be changed numerically without any intervention into the hardware. Two approaches of estimating velocity are considered. Finally, the system is implemented experimentally and the sound absorption performance is evaluated in the impedance tube.

2   Control methods

The knowledge of an analytical model of the actuator helps reduce the number of used sensors and consequently the cost of implementation of noise control system [9]. However, electroacoustic dynamics of the corona discharge depends on a number of medium properties such as humidity and ion mobility, which can vary during operation, making the development of actuator model and its implementation to real-time control an arduous task. Thus, pressure-velocity feedback method can be applied to control acoustic impedance in front of the CD actuator.

The absence of any moving part in the actuator poses some constraints on how the particle velocity can be estimated, as a laser velocimeter or accelerometer cannot be used. In this study the particle velocity is estimated with two different methods illustrated in Figure 1 and Figure 2 using a pair of microphones. Their relative performance is compared in the impedance tube in the next section. Since there are no acoustic sources between two microphones in Figure 1, velocity can be measured using one dimensional Euler equation. If the pressure gradient is approximated by a simple difference $(p_1 - p_2)/l$, the estimated velocity between the microphones can be written in frequency domain as:

$$v_{est} = \frac{p_1 - p_2}{\rho l s}, \tag{1}$$

where $s = j\omega$ is a Laplace variable, l is the separation between two microphones, ρ is the air density. The accuracy of velocity estimation depends on the ratio of the sound wavelength to distance between microphones: l should be fairly small compared to wavelength. However, if the wavelength is too large, the parasitic noise in the sensors can be greater than the actual pressure difference at positions p_1 and p_2. Thus, a compromise in a desired frequency range of operation should be found. The pressure measurement p_2 with desired acoustic impedance Z_{tg} (target impedance) defines the target velocity $v_{tg} = p_2/Z_{tg}$ that is needed in order to achieve Z_{tg} in front of the actuator. The difference between v_{tg} and v_{est} yields the error signal which should be minimized. The error is amplified by a dimensional gain G and forms a voltage u that applies to the actuator. Higher the gain, closer the achieved impedance should be to Z_{tg}. However in practice, there is always a limit above which the system becomes unstable. Rectangular blocks represent continuous-time transfer functions which should be discretised and implemented on a hardware. The transfer function $1/Z_{tg}$ is stable and proper. Within these requirements various complex frequency-dependent target impedances can be implemented.
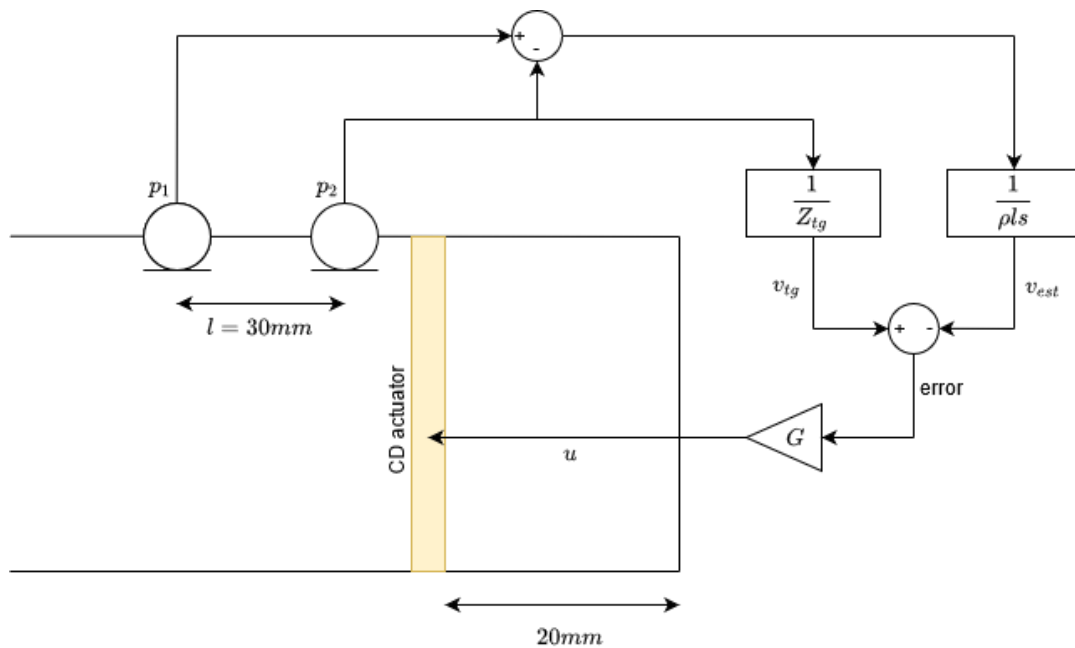
Figure 1. Scheme 1: pressure-velocity feedback impedance control schematic 1 for corona discharge actuator. Velocity is estimated with two microphones separated by 30 mm.

Figure 2 illustrates the control scheme similar to one mentioned above but with different approach to estimate particle velocity in front of the actuator. A thin porous layer, e.g. a wire mesh, with known flow resistance R is placed between the microphones. At low frequencies the particle velocity through a porous layer is controlled by its resistance [14]. Therefore, the estimation for acoustic velocity reads:

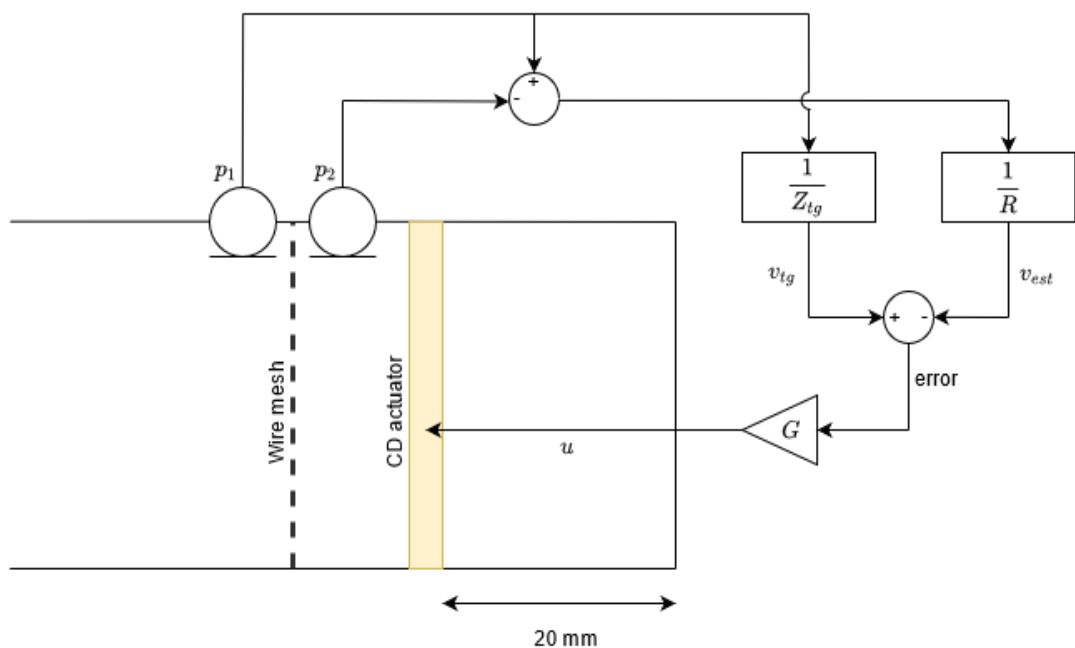$$v_{est} = \frac{p_1 - p_2}{R}. \tag{2}$$

Figure 2. Scheme 2: pressure-velocity feedback impedance control schematic 2 for corona discharge actuator. Velocity is estimated with two microphones separated by a wire mesh with resistance of $0.3\rho c$.

At high frequencies inertial forces become non-negligible reducing the accuracy of equation (2). In Figure 2 the target velocity is calculated with the use of microphone p_1 since the total impedance presented by an active absorber is the one on the front face of the wiremesh.

Target acoustic impedance can be changed digitally in the controller that allows adjusting the system to optimal absorption in various configurations. Moreover, since it is possible to set a complex frequency-dependent impedance, this method is advantageous compared to the hybrid absorption method under grazing incidence [8][13].

3 Implementation and achieved absorption

This section presents an overview of corona discharge actuator used in the laboratory measurements, experimental setup and achieved performance of impedance control with two methods of velocity estimation.

3.1 Corona discharge actuator

The corona discharge actuator prototype is built in a wire-to-mesh geometry (Figure 3). The frame with 50x50 mm^2 hollow area is manufactured on a 3D printer from PLA plastic. The high voltage electrode is made from a single 0.1 mm in diameter nichrome wire which passes five times the internal area. All parts of high voltage wire are parallel and separated by 10 mm forming a plane. The grounded electrode is made from a stainless steel perforated plate which is fixed parallel to high voltage electrode plane at the distance of 6 mm. Due to the coarse perforation, the plate presents negligible acoustic resistance and thus is almost transparent to sound. In this configuration a stable positive corona discharge can be formed, at atmospheric conditions, within the voltage range ~6-10 kV with interelectrode current up to 1 mA. When a constant positive voltage is applied to the high voltage electrode, positive ions are generated close to it and drift towards the grounded plate. In the interelectrode volume ions elastically interact with the neutral air particles transferring mechanical momentum and consequently creating the air flow. Part of total energy locally releases in the form of heat. If the constant voltage is superimposed with alternating one, the modulation of airflow and heat release finally creates a sound wave. For more details, refer to [12].
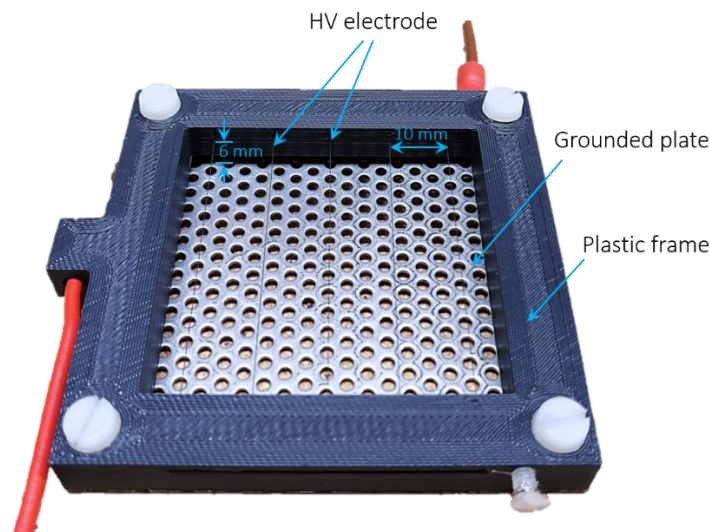

Figure 3. Photo of corona discharge actuator in a wire-to-mesh geometry used in this study.

3.2 Experimental setup

To evaluate the absorption performance of the impedance control methods with CD actuator, the measurements under normal sound incidence are performed in the impedance tube. The length of the tube is 1.1 m, cross section is 50x50 mm². The actuator is backed by rectangular enclosure with 50x50 mm² cross section and 20

mm depth and fixed at one termination of the impedance tube. A 10 mm-thick layer of melamine foam is fixed at the enclosure termination in order to increase control stability (due to sound reflections on the back wall). Such dimensions allow to study absorption qualities under normal plane wave incidence at frequencies below 3 kHz. The termination at the left is closed by a loudspeaker used to generate bidirectional sinusoidal sweep. Microphones M_1 and M_2 placed 50 mm apart assess acoustic impedance and absorption coefficient of CD-based active absorber according to ISO-10534-2 standard [15]. Signals from these microphones are processed with Brüel&Kjaer Pulse frequency analyzer.

The hardware used to control the CD actuator is depicted at the right in Figure 4. A pair of PCB130D20 quarter inch microphones sense the pressure at positions p_1 and p_2. The control schemes from Figure 1 and Figure 2 are implemented in real-time platform Speedgoat IO-334. The discretised loop runs at frequency 50 kHz. As the controller cannot generate high voltage, the following procedure is performed. The voltage calculated by controller to supply the actuator (in the range of kV) is reduced by a factor 1000 before the output. Controller is then connected to TREK 615–10 high voltage AC/DC amplifier (±10 kV, 10 mA) which amplifies the signal back by 1000 and supplies the actuator.

The performance of the active absorber is evaluated in the frequency range 100 – 2000 Hz so that the lower limit is higher than the cut off frequency of the control microphones (50 Hz) and the higher limit is sufficiently lower than the sampling rate of the controller. Therefore, to estimate velocity in scheme 1 the separation $l =30$ mm was chosen as a compromise to keep the sound absorbing system small and work in the considered frequency range. When v_{est} is measured according to scheme 2, the wire mesh with thickness of 0.3 mm and flow resistance $R = 0.3\rho c$ is installed, $l =9$ mm.
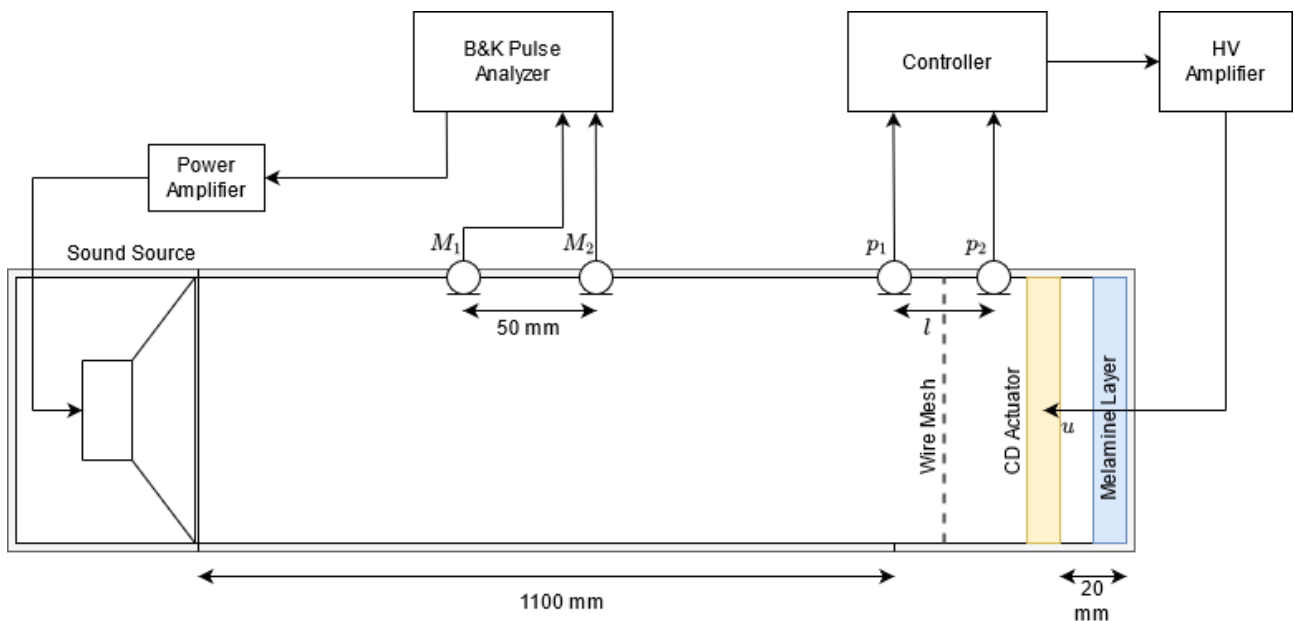

Figure 4. The schematic of experimental setup. The impedance control system is depicted on the right. To implement scheme 1, wire mesh is removed, $l = 30$ mm. To implement scheme 2, wiremesh is installed, $l = 9$ mm. Not to scale.

3.3 Achieved impedance and sound absorption

Performance of plasma-based sound absorber is evaluated sequentially for two approaches of particle velocity estimation. The measurements are carried out in the same environmental conditions and levels of sound source excitation. The feedback gain G in both cases is set the highest before the control system becomes unstable. The target impedance is set to $Z_{tg} = \rho c \approx 418$ Pa·s/m in order to aim the maximal absorption in the impedance tube. Figure 5 represents the performance of the active system in terms of achieved impedance in comparison

with passive operation. For scheme 1 the plane of impedance measurement is positioned in the middle between the two control microphones; for scheme 2 it is located at the front face of the wire mesh. When the actuator is not controlled (passive case), the low frequency behaviour in both scheme 1 and scheme 2 (dashed lines) is mostly governed by the stiffness of the actuator enclosure. It leads to high magnitudes and negative phase of measured impedance. At frequencies above 1000 Hz the trends are rather different for two installations since the impedance measurement is carried out at slightly different distances from the back wall, and additional resistive wire mesh is installed in scheme 2. When the control is on (solid lines in Figure 5), the impedance magnitude in both cases drops to values much closer to ρc, than in passive operation. The phase of the impedance shifts closer towards zero, since target impedance is purely real. In the range from 1 kHz the actively achieved impedance tends closer to the passive values. This can mean that the control either loses its efficiency or the passive absorption increases towards high frequencies and strong control action is not needed anymore. In passive case for scheme 2 (dashed orange line) it is visible that the impedance magnitude and phase are relatively close to Z_{tg} towards 2000 Hz. Bottom line, the acoustic impedance is both active cases moves towards $Z_{tg} = \rho c$ in the whole frequency range considered.
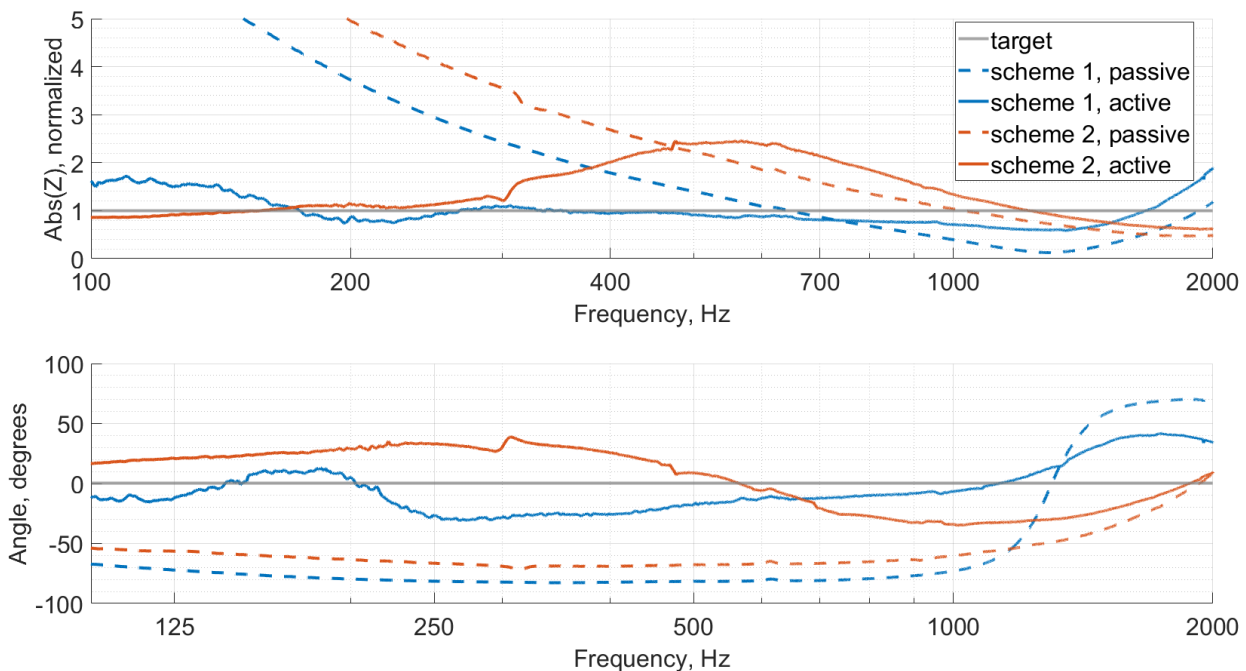

Figure 5. Frequency responses of acoustic impedances measured for scheme 1 (blue lines) and scheme 2 (orange lines) in two cases: the actuator is supplied only with DC voltage (passive, dashed lines), and the actuator is controlled (active, solid lines). Magnitude is normalized by ρc.

The analysis of acoustic impedance above is supported by the achieved sound absorption shown in Figure 6. At low frequencies, the passive systems almost do not absorb sound. In scheme 1 all passive absorption is provided by a 10 mm melamine layer. Thus, it reaches only 50% at 2000 Hz. In scheme 2 additional resistive wire mesh transforms passive system to a quarter wavelength resonator with size of approximately 40 mm, which substantially increases absorption at higher frequencies. However, it does not reach perfect absorption as the mesh resistance is not matched to ρc.

Both active schemes reach absorption values higher than 0.8 in the whole considered frequency range which proves the efficiency of the concept to use CD actuator as the controlled source. It can be seen, that sound absorption gradually decreases for scheme 1 (blue solid line in Figure 6) above 1000 Hz. Authors suggest that it can be the result of growing error in v_{est} as the sound wavelength decreases compared to microphone separation making linear approximation of pressure gradient less accurate. Absorption performance of active absorber in scheme 2 (orange solid line in Figure 6) also locally decreases till 500 Hz. Since the assumption

of purely resistive wire mesh is valid only at low frequencies, the increasing error in v_{est} can be the reason of such dynamics. At higher frequencies this effect is compensated by growing passive absorption of the system. Therefore, velocity estimation through the Euler equation (1) (used in scheme 1) leads to a slightly higher absorption at frequencies from 250 Hz to 1150 Hz than with the second approach. Above this, up to 2000 Hz, the system with a wiremesh performs better. In the low frequency range both approaches provide absorption more than 90%. Nevertheless, the achieved bandwidth of effective absorption covers the whole studied range from 100 Hz to 2000 Hz and can be possibly extended to lower frequencies with different control microphones.
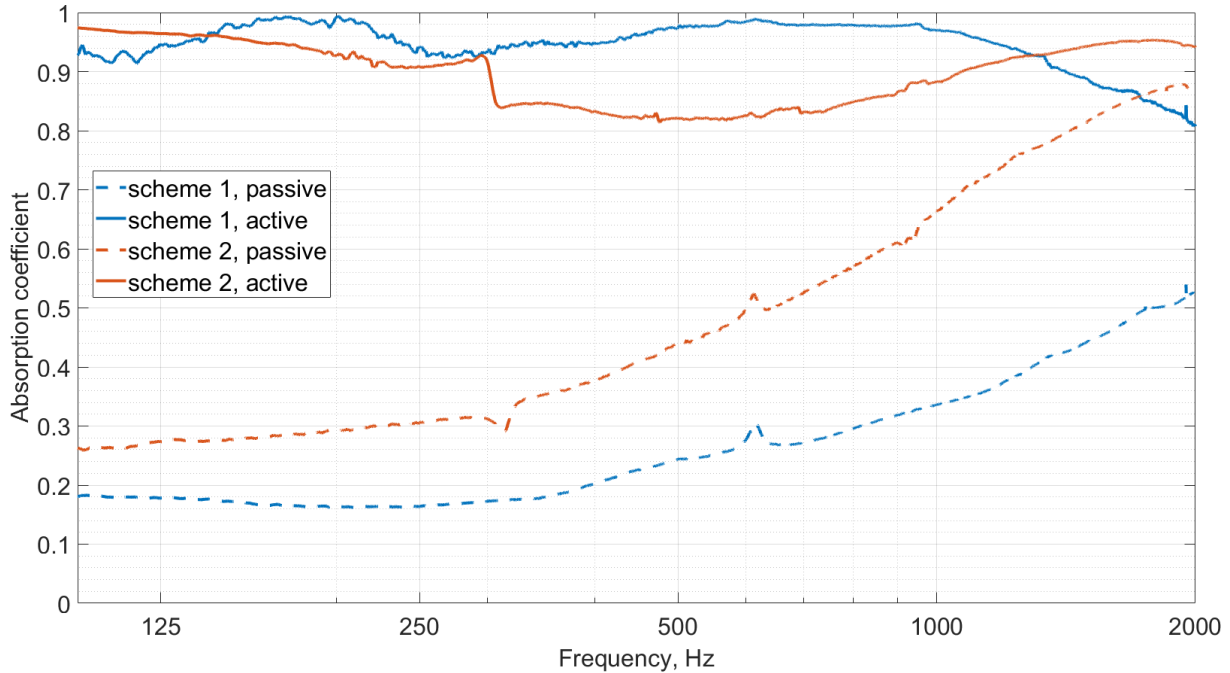

Figure 6. Sound absorption coefficient calculated for scheme 1 (blue lines) and scheme 2 (orange lines) in two cases: the actuator is supplied only with DC voltage (passive, dashed lines), and the actuator is controlled (active, solid lines).

4 Conclusions

In this study the application of active acoustic impedance control method to an electroacoustic actuator based on corona discharge is presented. Specifically, pressure-velocity feedback approach is implemented since the model of the actuator is unknown. Estimation of particle velocity is performed in two ways using two microphones: based on the Euler equation, and based on low frequency approximation of flow velocity through a resistive layer. The absorber performance is evaluated in the impedance tube under normal incidence.
The achieved sound absorption remains higher than 80 % in the frequency range from 100 to 2000 Hz.
The motivation to use the plasma-based actuators in active noise control consists in their simple, flexible, and mechanically robust design. Porous electrodes make the transducer transparent for sound and flow. In contrast to conventional loudspeakers, where the presence of acoustic mass and stiffness cannot be completely mitigated [9], the CD actuator does not present any resonant behaviour. As a consequence, it does not impose any additional physical limitation on the control performance and allows achieving greater bandwidth of effective absorption as demonstrated in this work. On the other side, the voltage range that can be applied to the actuator is bounded between the beginning of ionization process and transition to a continuous arc. Therefore, a particular CD actuator has a limit on the output power which is not straightforward to overcome. Compared to a hybrid absorption strategy, the direct impedance control provides flexibility in change of the target impedance assuming the closed loop transfer function is stable, which makes this approach attractive for grazing incidence absorption. Although in scheme 2 the impedance presented by the passive wire mesh

should be taken into account (it limits the lower resistance to aim), the system appeared to be more compact than in scheme 1 which needs greater microphone separation for accurate measurements.

The performance of the active feedback impedance control strategy with the use of the CD actuator reveals a great potential of this transducer for active control purposes.

Acknowledgements

References

[1] Chakravarthy, S. R., & Kuo, S. M. (2006, May). Application of active noise control for reducing snore. In *2006 IEEE International Conference on Acoustics Speech and Signal Processing Proceedings* (Vol. 5, pp. V-V). IEEE.

[2] Molesworth, B. R., Burgess, M., & Chung, A. (2013). Using active noise cancelling headphones to reduce the effects of masking in commercial aviation. *Acta Acustica united with Acustica*, *99*(5), 822-827.

[3] Cong, C., Tao, J., & Qiu, X. (2018). A multi-tone sound absorber based on an array of shunted loudspeakers. *Applied Sciences*, *8*(12), 2484.

[4] E. Rivet. *Room modal equalisation with electroacoustic absorbers.* Ph.D. thesis, Ecole Polytechnique Fédérale de Lausanne, 2016.

[5] Kajikawa, Y., Gan, W. S., & Kuo, S. M. (2013, September). Recent applications and challenges on active noise control. In *2013 8th International Symposium on Image and Signal Processing and Analysis (ISPA)* (pp. 661-666). IEEE.

[6] Mirshekarloo, M. S., Tan, C. Y., Yu, X., Zhang, L., Chen, S., Yao, K., ... & Tan, S. T. (2018). Transparent piezoelectric film speakers for windows with active noise mitigation function. *Applied Acoustics*, *137*, 90-97.

[7] Billon, K., De Bono, E., Perez, M., Salze, E., Matten, G., Gillet, M., ... & Collet, M. (2021, March). Experimental assessment of an active (acoustic) liner prototype in an acoustic flow duct facility. In *Health Monitoring of Structural and Biological Systems XV* (Vol. 11593, p. 115932L). International Society for Optics and Photonics.

[8] Betgen, B., Galland, M. A., Piot, E., & Simon, F. (2012). Implementation and non-intrusive characterization of a hybrid active–passive liner with grazing flow. *Applied Acoustics*, *73*(6-7), 624-638.

[9] Rivet, E., Karkar, S., & Lissek, H. (2016). Broadband low-frequency electroacoustic absorbers through hybrid sensor-/shunt-based impedance control. *IEEE Transactions on Control Systems Technology*, *25*(1), 63-72.

[10] Moreau, E. (2007). Airflow control by non-thermal plasma actuators. *Journal of physics D: applied physics*, *40*(3), 605.

[11] Bastien, F. (1987). Acoustics and gas discharges: applications to loudspeakers. *Journal of Physics D: Applied Physics*, *20*(12), 1547.

[12] Sergeev, S., Lissek, H., Howling, A., Furno, I., Plyushchev, G., & Leyland, P. (2020). Development of a plasma electroacoustic actuator for active noise control applications. *Journal of Physics D: Applied Physics*, *53*(49), 495202.

[13] Sergeev, S., & Lissek, H. (2020, December). Corona discharge actuator for active sound absorption. In *Forum Acusticum* (pp. 1551-1555).

[14] Furstoss, Marc, Denis Thenail, and Marie-Annick Galland. "Surface impedance control for sound absorption: direct and hybrid passive/active strategies." *Journal of sound and vibration* 203.2 (1997): 219-236.

[15] Acoustics—Determination of Sound Absorption Coefficient and Impedance in Impedance Tubes—Part 2: Transfer-Function Method, Standard ISO 10534-2:1998, ISO, Geneva, Switzerland, 1998